Geophys. J. Int. (2009) **179,** 459–474 doi: 10.1111/j.1365-246X.2009.04305.x

An implicit staggered-grid finite-difference method for seismic modelling

Yang Liu[1,2] and Mrinal K. Sen[2]

[1]*State Key Laboratory of Petroleum Resource and Prospecting, China University of Petroleum, Beijing, Beijing,* 102249*, China.*
E-mail: wliuyang@vip.sina.com
[2]*The Institute for Geophysics, John A. and Katherine G. Jackson School of Geosciences, The University of Texas at Austin,* R2200 *Austin,* TX 78758*, USA*

Accepted 2009 June 19. Received 2009 May 21; in original form 2008 December 2

SUMMARY

We derive explicit and new implicit staggered-grid finite-difference (FD) formulas for derivatives of first order with any order of accuracy by a plane wave theory and Taylor's series expansion. Furthermore, we arrive at a practical algorithm such that the tridiagonal matrix equations are formed by the implicit FD formulas derived from the fractional expansion of derivatives. Our results demonstrate that the accuracy of a $(2N + 2)$th-order implicit formula is nearly equivalent to or greater than that of a $(4N)$th-order explicit formula. The new implicit method only involves solving tridiagonal matrix equations. We also demonstrate that a $(2N + 2)$th-order implicit formulation requires nearly the same amount of memory and computation as those of a $(2N + 4)$th-order explicit formulation but attains the accuracy achieved by a $(4N)$th-order explicit formulation when additional cost of visiting arrays is not considered. Our analysis of efficiency and numerical modelling results for elastic wave propagation demonstrates that a high-order explicit staggered-grid method can be replaced by an implicit staggered-grid method of some order, which will increase the accuracy but not the computational cost.

Key words: Numerical solutions; Computational seismology; Wave propagation.

GJI Seismology

1 INTRODUCTION

Numerical simulation of seismic wave propagation is carried out using standard methods of solving partial differential equations that appear in different branches of science and engineering. Finite difference (FD) and finite elements (FE) are the two most widely used numerical approaches. Although the FE methods based on spectral element (e.g. Komatitsch & Vilotte 1998; De Basabe & Sen 2007) and discontinuous Galerkin (e.g. Rivière & Wheeler 2003; Käser & Dumbser 2006; De Basabe *et al.* 2008) methods are being investigated aggressively by the seismological community, FD-based methods still remain very popular due to the ease of their implementation. Although the high-order FE methods offer greater stability and grid dispersion properties, they are generally computationally more expensive (De Basabe & Sen 2009).

The application of FD methods for seismic modelling (e.g. Kelly *et al.* 1976; Dablain 1986; Virieux 1986; Igel *et al.* 1995; Aoi & Fujiwara 1999; Pitarka 1999; Vossen *et al.* 2002; Etgen & O'Brien 2007; Saenger *et al.* 2007; Rojas *et al.* 2008), migration (e.g. Claerbout 1985; Larner & Beasley 1987; Li 1991; Ristow & Ruhl 1994; Zhang *et al.* 2000) and inversion (e.g. Pratt *et al.* 1998; Ravaut *et al.* 2004; Fei & Liner 2008; Abokhodair 2009) can be found in numerous papers. To improve the accuracy and stability of FD method in numerical modelling, many variants of the methods have been proposed—these include difference schemes of variable grid (Wang & Schuster 1996; Hayashi & Burns 1999), irregular grid (Opršal & Zahradník 1999), variable time step (Tessmer 2000) and high-order accuracy (Dablain 1986; Fornberg 1987; Crase 1990; Hestholm 2007; Liu & Wei 2008).

Compared with the conventional-grid FD methods, staggered-grid FD methods have greater precision and better stability and have been widely used in seismic modelling (e.g. Madariaga 1976; Virieux 1984, 1986; Levander 1988; Graves 1996; Gottschämer & Olsen 2001; Mittet 2002; Moczo *et al.* 2002; Bohlen & Saenger 2006). Stability and grid dispersion in the 3-D fourth-order displacement-stress staggered-grid FD scheme have been investigated by Moczo *et al.* (2000). Staggered-grid FD modelling can also be performed with models including surface topography (e.g. Ohminato & Chouet 1997; Hestholm & Ruud 1998; Hestholm 2003; Lombard *et al.* 2008). Viscoacoustic and viscoelastic wave modelling using staggered-grid FDs have also been studied and reported in recent years (e.g. Robertsson *et al.* 1994; Robertsson 1996; Hayashi *et al.* 2001; Bohlen 2002). A frequency-domain staggered-grid FD method has also been developed to model 3-D viscoacoustic wave propagation (Operto *et al.* 2007).

Saenger *et al.* (2000) derived a new rotated staggered-grid scheme in which all medium parameters are defined at appropriate positions within an elementary cell for the essential operations. Using this modified grid, it is possible to simulate the propagation of elastic waves in a

medium containing cracks, pores or free surfaces (Saenger & Shapiro 2002); anisotropy (Saenger & Bohlen 2004; Bansal & Sen 2008) and scattering and diffraction by a single crack (Krüger *et al.* 2005).

Although a few results on implicit FD methods with standard grids are available, most common FD methods are explicit. To yield modelling results with an increased accuracy, implicit FD formulas have been developed for the elastic wave equation (Emerman *et al.* 1982). These formulas express the value of a variable at some point at a future time in terms of the value of the variable at that point and at neighbouring points at present time, past times and future times. An implicit method for time derivatives has also been used in seismic migration (e.g. Ristow & Ruhl 1997; Shan 2007; Zhang & Zhang 2007). One other example of an implicit method is a compact finite-difference method (CFDM, Lele 1992). Many reports have been published on this method but it is seldom utilized in geophysics. The method, however, has been widely studied and applied in other areas (e.g. Ekaterinaris 1999; Meitz & Fasel 2000; Lee & Seo 2002; Nihei & Ishii 2003). Kosloff *et al.* (2008) developed a new implicit numerical scheme for the solution of the constant-density acoustic wave equation using standard grid FDs. The scheme is based on recursive second-derivative operators and involves the solution of a tridiagonal linear system of equations.

In this paper, we report on the development of efficient space derivative operators using a staggered-grid scheme. An explicit staggered-grid finite-difference method (ESFDM) directly calculates the derivative value at some point in terms of the function values at its neighbouring points. However, an implicit staggered-grid finite-difference method (ISFDM) expresses the derivative value at some point in terms of both the function values and the derivative values at its neighbouring points. Therefore, it involves solving a set of linear equations to obtain the derivative values. Boersma (2005) presented a compact high-order (up to 12th order) staggered CFDM, a kind of implicit method, to solve the compressible Navier–Stokes equations.

In this paper, we derive both explicit and implicit staggered-grid FD formulas with even-order accuracy for first-order derivatives. Our approach has close similarities with that adopted in Kosloff *et al.* (2008); however, we differ significantly in the details of the implementation in that unlike second-order derivative operators derived by Kosloff *et al.* (2008) for acoustic wave equation with second-order spatial derivatives, we develop the operators for staggered-grid FDs. These can be used to solve acoustic and elastic wave equations with first-order spatial derivatives in heterogeneous media using staggered grids. First, we describe our method of derivation of implicit operators and a scheme for their efficient implementation. We compare their accuracy with dispersion analysis and finally demonstrate some results of numerical modelling using a realistic 2-D elastic model. Numerical accuracy of our result is compared with that of a pseudospectral method (PSM; accurate to infinite order). Our results show that the implicit method of some order can reach the accuracy of some higher-order explicit method but cost less computation time and thus demonstrate the validity and efficiency of the new implicit method.

2 EXPLICIT AND IMPLICIT STAGGERED-GRID FD FORMULA WITH EVEN-ORDER ACCURACY

2.1 (2*N*)th-order explicit staggered-grid FD formula

An explicit staggered-grid FD formula for a function $p(x)$ is defined as follows (Kindelan *et al.* 1990):

$$\frac{\partial p}{\partial x} \approx \frac{\delta p}{\delta x} = \frac{1}{h}\sum_{n=1}^{N} c_n \left[p(x+nh-0.5h) - p(x-nh+0.5h)\right], \tag{1}$$

where x is a real variable, h is a small value, N is a positive integer and c_n are FD coefficients.

Let

$$p = p_0 e^{ikx} \tag{2a}$$

and

$$\beta = kh/2, \tag{2b}$$

where k is the wavenumber, $i = \sqrt{-1}$ and p_0 is a constant. Using eqs (2a) and (2b), eq. (1) becomes

$$\beta \approx \sum_{n=1}^{N} c_n \sin\left[(2n-1)\beta\right]. \tag{3}$$

Using a Taylor's series expansion, we have

$$\beta \approx \sum_{m=1}^{\infty}\left[\frac{(-1)^{m-1}}{(2m-1)!}\sum_{n=1}^{N}(2n-1)^{2m-1} c_n \beta^{2m-1}\right]. \tag{4}$$

Comparing β coefficients, we obtain

$$\frac{(-1)^{m-1}}{(2m-1)!}\sum_{n=1}^{N}\left[(2n-1)^{2m-1}\right] c_n = \begin{cases} 1 & (m=1) \\ 0 & (m=2,3,\ldots,N) \end{cases}. \tag{5}$$

Table 1. Coefficients of the explicit staggered-grid finite-difference formulas.

Order of accuracy	c_1	c_2	c_3	c_4	c_5	c_6
2	1					
4	9/8	−1/24				
6	75/64	−25/384	3/640			
8	1225/1024	−245/3072	49/5120	−5/7168		
10	19 845/16384	−735/8192	567/40 960	−405/229 376	35/294 912	
12	160 083/131 072	−12 705/131 072	22 869/1 310 720	−5445/1 835 008	847/2 359 296	−63/2 883 584

Eq. (5) can be rewritten in the following matrix form:

$$\begin{bmatrix} 1^0 & 3^0 & \cdots & (2N-1)^0 \\ 1^2 & 3^2 & \cdots & (2N-1)^2 \\ \vdots & \vdots & \vdots & \vdots \\ 1^{2N-2} & 3^{2N-2} & \cdots & (2N-1)^{2N-2} \end{bmatrix} \begin{bmatrix} 1c_1 \\ 3c_2 \\ \vdots \\ (2N-1)c_N \end{bmatrix} = \begin{bmatrix} 1 \\ 0 \\ \vdots \\ 0 \end{bmatrix}. \tag{6}$$

Its coefficient matrix is a Vandermonde matrix. For the Vandermonde matrix $\mathbf{A} = [a_{jm}\ ]_{n\times n} = [x_j^m\ ]_{n\times n}$, its determinant equals $\prod_{1\le j<m\le n}(x_m - x_j)$ (Meyer 2000). Therefore, the $c_n (n = 1, 2, \ldots, N)$ values are obtained as follows by solving eq. (6):

$$c_n = \frac{(-1)^{n+1}}{2n-1} \prod_{1\le m\le N, m\ne n} \left| \frac{(2m-1)^2}{(2n-1)^2 - (2m-1)^2} \right|. \tag{7}$$

These coefficients are equivalent to those obtained by Pei (2004). The coefficients, listed in Table 1 from 2nd-order to 12th-order accuracy, are the same as those for 4th-order to 8th-order accuracy obtained by Kindelan *et al.* (1990).

The absolute error of the explicit FD formulas, derived from eq. (4), is as follows:

$$\begin{aligned} e_N &= \sum_{m=N+1}^{\infty} \left[\frac{(-1)^{m-1}}{(2m-1)!} \sum_{n=1}^{N} (2n-1)^{2m-1} c_n \beta^{2m-1} \frac{2}{h} \right] \\ &= \sum_{m=N+1}^{\infty} \left[\frac{(-1)^{m-1} k^{2m-1}}{2^{2m-2}(2m-1)!} \sum_{n=1}^{N} (2n-1)^{2m-1} c_n h^{2m-2} \right]. \end{aligned} \tag{8}$$

The minimum power of h in the error function is $2N$; therefore, the explicit FD formula (1) has $(2N)$th-order accuracy.

2.2 $(2N + 2)$th-order implicit staggered-grid FD formula

To derive the implicit FD formula, we introduce Claerbout's (1985) idea first.

The second-order difference operator for a function $p(x)$ is expressed as

$$\frac{\partial^2 p}{\partial x^2} \approx \frac{\delta^2 p}{\delta x^2} = \frac{p(x+h) + p(x-h) - 2p(x)}{h^2}. \tag{9}$$

The following expression is introduced by adding higher-order terms to improve the accuracy of FD:

$$\frac{\partial^2 p}{\partial x^2} \approx \frac{\delta^2 p}{\delta x^2} - b\frac{\delta^4 p}{\delta x^4}, \tag{10}$$

where b is an adjustable constant. This expression is hardly ever used and is suggested to be changed as follows (Claerbout 1985):

$$\frac{\partial^2 p}{\partial x^2} \approx \frac{\dfrac{\delta^2 p}{\delta x^2}}{1 + b\dfrac{\delta^2}{\delta x^2}}. \tag{11}$$

This equation provides a higher precision than eq. (9). Motivated by this idea, an implicit staggered-grid FD formula is defined as follows:

$$\frac{\partial p}{\partial x} \approx \frac{\dfrac{\delta p}{\delta x}}{1 + bh^2\dfrac{\delta^2}{\delta x^2}} = \frac{\dfrac{1}{h}\displaystyle\sum_{n=1}^{N} c_n \left[p(x + nh - 0.5h) - p(x - nh + 0.5h) \right]}{1 + bh^2\dfrac{\delta^2}{\delta x^2}}. \tag{12}$$

Substituting $p = p_0\, e^{ikx}$ and $\beta = kh/2$ into eq. (12) and simplifying it, we have

$$\left[1 - 2b + 2b\cos(2\beta)\right]\beta \approx \sum_{n=1}^{N} c_n \sin\left[(2n-1)\beta\right]. \tag{13}$$

Table 2. Coefficients of the implicit staggered-grid finite-difference formulas.

Order of accuracy	b	c_1	c_2	c_3	c_4	c_5
4	1/24	1				
6	9/80	63/80	17/240			
8	25/168	2675/4032	925/8064	−61/40 320		
10	49/288	64 925/110 592	78 841/552 960	−343/110 592	43/430 080	
12	81/440	96 579/180 224	364 119/2 252 800	−70 821/15 769 600	15 957/63 078 400	−221/22 708 224

Using the Taylor's series expansion, we obtain

$$\left[1+2b\sum_{m=1}^{\infty}(-1)^m\frac{2^{2m}}{(2m)!}\beta^{2m}\right]\beta\approx\sum_{m=1}^{\infty}\left[\frac{(-1)^{m-1}}{(2m-1)!}\sum_{n=1}^{N}(2n-1)^{2m-1}c_n\beta^{2m-1}\right]. \tag{14}$$

Comparing β coefficients, we get

$$\frac{(-1)^{m-1}}{(2m-1)!}\sum_{n=1}^{N}\left[(2n-1)^{2m-1}c_n\right]=\begin{cases}1 & (m=1)\\ \dfrac{(-1)^{m-1}2^{2m-1}}{(2m-2)!}b & (m=2,3,\ldots,N+1)\end{cases}. \tag{15}$$

We can rewrite eq. (15) in the following matrix form:

$$\begin{bmatrix}1^0 & 3^0 & \cdots & (2N-1)^0 & 0\\ 1^2 & 3^2 & \cdots & (2N-1)^2 & -(2\times1+1)\,2^{(2\times1+1)}\\ \vdots & \vdots & \vdots & \vdots & \vdots\\ 1^{2N} & 3^{2N} & \cdots & (2N-1)^{2N} & -(2\times N+1)\,2^{(2\times N+1)}\end{bmatrix}\begin{bmatrix}1c_1\\ 3c_2\\ \vdots\\ (2N-1)\,c_N\\ b\end{bmatrix}=\begin{bmatrix}1\\0\\ \vdots\\0\end{bmatrix}. \tag{16}$$

The $c_m (m=1,2,\ldots,N)$ and b values are obtained by solving these equations.

The absolute error of the implicit FD formula, derived from eq. (14), is as follows:

$$\begin{aligned}e_N&=2b\sum_{m=N+1}^{\infty}(-1)^m\frac{2^{2m}}{(2m)!}\beta^{2m+1}\frac{2}{h}-\sum_{m=N+2}^{\infty}\left[\frac{(-1)^{m-1}}{(2m-1)!}\sum_{n=1}^{N}(2n-1)^{2m-1}c_n\beta^{2m-1}\frac{2}{h}\right]\\&=\sum_{m=N+1}^{\infty}\frac{(-1)^m k^{2m+1}}{(2m)!}\left[2b-\frac{1}{2^{2m}(2m+1)}\sum_{n=1}^{N}(2n-1)^{2m+1}c_n\right]h^{2m}.\end{aligned} \tag{17}$$

The minimum power of h in the error function is $2N+2$; therefore, the implicit FD formula (12) has $(2N+2)$th-order accuracy.

For $N=2$, eq. (16) becomes

$$\begin{bmatrix}1 & 1 & 0\\ 1 & 9 & -24\\ 1 & 81 & -160\end{bmatrix}\begin{bmatrix}c_1\\ 3c_2\\ b\end{bmatrix}=\begin{bmatrix}1\\0\\0\end{bmatrix}. \tag{18}$$

Solving these equations, we get $b=9/80$, $c_1=63/80$ and $c_2=17/240$. The coefficients of implicit staggered difference from 4th-order to 12th-order accuracy are listed in Table 2.

3 COMPARISON OF ACCURACY BETWEEN IMPLICIT AND EXPLICIT STAGGERED-GRID FD FORMULAS

Since our goal is to satisfy eqs (3) and (13), we examine the following functions to investigate the accuracy of these formulas:

$$f_{\mathrm{ESFDM}}(\beta)=\sum_{n=1}^{N}c_n\sin\left[(2n-1)\,\beta\right] \tag{19}$$

and

$$f_{\mathrm{ISFDM}}(\beta)=\frac{\displaystyle\sum_{n=1}^{N}c_n\sin\left[(2n-1)\,\beta\right]}{1-2b+2b\cos(2\beta)}. \tag{20}$$

The FD coefficients of ESFDM are obtained from eq. (6) and those of ISFDM are obtained from eq. (16). The calculated $f_{\mathrm{ESFDM}}(\beta)$ and $f_{\mathrm{ISFDM}}(\beta)$ are compared with β for different orders. Figs 1(a) and (b) show dispersion functions $f_{\mathrm{ESFDM}}(\beta)/\beta$ and $f_{\mathrm{ISFDM}}(\beta)/\beta$ with different

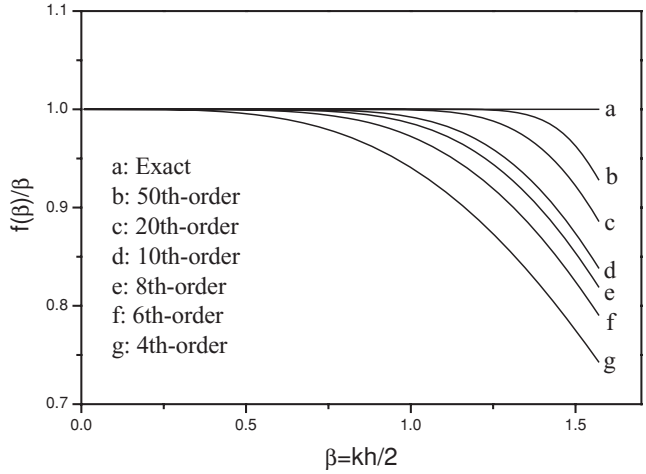

(a) $f_{\mathrm{ESFDM}}(\beta)/\beta$ of ESFDM with different orders

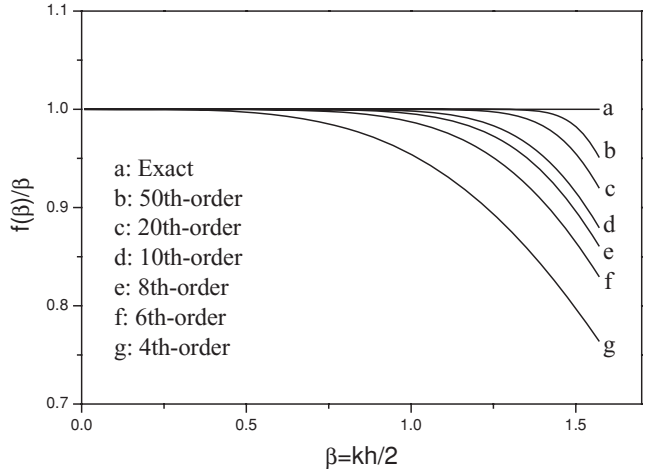

(b) $f_{\mathrm{ISFDM}}(\beta)/\beta$ of ISFDM with different orders

Figure 1. Plot of $f_{\mathrm{ESFDM}}(\beta)/\beta$ and $f_{\mathrm{ISFDM}}(\beta)/\beta$ with different orders. (a) $f_{\mathrm{ESFDM}}(\beta)/\beta$ of ESFDM with different orders. (b) $f_{\mathrm{ISFDM}}(\beta)/\beta$ of ISFDM with different orders.

orders and indicate that the accuracy of ESFDM and ISFDM increases with the increase of order. The accuracy of ISFDM is greater than that of ESFDM for the same order. The variations of $f_{\mathrm{ISFDM}}(\beta)/\beta$ and $f_{\mathrm{ESFDM}}(\beta)/\beta$ with β demonstrate that both $f_{\mathrm{ISFDM}}(\beta)$ and $f_{\mathrm{ESFDM}}(\beta)$ are increasing functions and that their values are not greater than β when β varies from 0 to $\pi/2$. Therefore, an error function is introduced as the following to quantitatively evaluate their accuracies:

$$e_f = \frac{1}{n+1} \sum_{\beta=0,\Delta\beta,2\Delta\beta,\ldots,n\Delta\beta} |\beta - f(\beta)|. \tag{21}$$

The errors of $f_{\mathrm{ESFDM}}(\beta)$ and $f_{\mathrm{ISFDM}}(\beta)$ are calculated and shown in Fig. 2 when $\Delta\beta = 0.001$ and $n = 1570$. The results indicate that the error of ISFDM is less than that of ESFDM for the same order. Letting (N_{E})th-order ESFDM have nearly the same error as (N_{I})th-order ISFDM, we find a relationship between N_{E} and N_{I}, that is, ($4N$)th-order ESFDM for $2N + 2 < 8$, ($4N + 2$)th-order ESFDM for $2N + 2 < 20$, (4N + 4)th-order ESFDM for $2N + 2 < 32$, ($4N + 6$)th-order ESFDM for $2N + 2 < 44$, ($4N + 8$)th-order ESFDM for $2N + 2 < 56$ and ($4N + 10$)th-order ESFDM for $2N + 2 < 68$ have nearly the same errors as ($2N + 2$)th-order ISFDM. These relationships are listed in Table 3.

We calculate both $f_{\mathrm{ISFDM}}(\beta)/\beta$ and $f_{\mathrm{ESFDM}}(\beta)/\beta$, with the order varying from 4 to 60 and 4 to 120, respectively. Fig. 3 shows $f_{\mathrm{ESFDM}}(\beta)/\beta$ and $f_{\mathrm{ISFDM}}(\beta)/\beta$ with nearly the same accuracy in each figures. We find that the accuracy of ($2N + 2$)th-order implicit formulas is equivalent to or greater than that of ($4N$)th-order explicit formulas, which is also shown in Table 3.

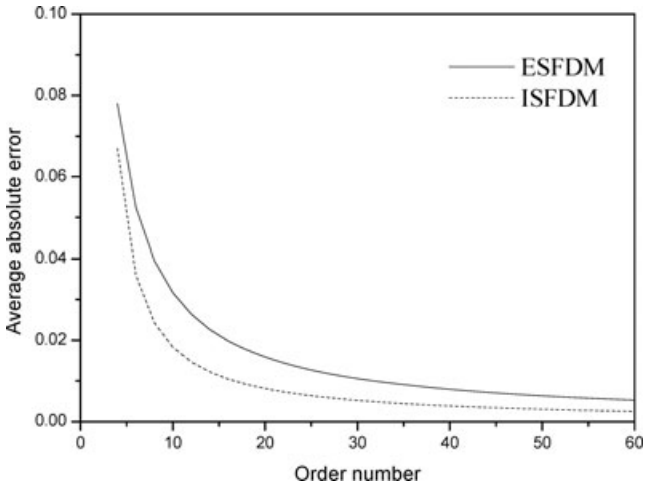

Figure 2. Errors of ESFDM and ISFDM for different orders.

Table 3. Order of ISFDM and ESFDM with the same accuracy.

Order of ISFDM	Order of ESFDM
$2N+2$: 4∼6	$4N$: 4∼8
$2N+2$: 8∼18	$4N+2$: 14∼34
$2N+2$: 20∼30	$4N+4$: 40∼60
$2N+2$: 32∼42	$4N+6$: 66∼86
$2N+2$: 44∼54	$4N+8$: 92∼112
$2N+2$: 56∼66	$4N+10$: 118∼138

4 A TRIDIAGONAL SYSTEM FOR THE IMPLICIT STAGGERED-GRID FD METHOD

Let $q = \partial p/\partial x$ and using eq. (12), the implicit staggered-grid FD formula of $(2N+2)$th-order is expressed as

$$bq(x-h) + (1-2b)q(x) + bq(x+h) = \frac{1}{h}\sum_{m=1}^{N} c_m \left[p(x+mh-0.5h) - p(x-mh+0.5h)\right]. \tag{22}$$

This formula reduces to a $(2N)$th-order explicit staggered-grid FD formula when $b = 0$. For implicit format, $b \neq 0$, let

$$a = \frac{1}{b} - 2 \tag{23a}$$

and

$$r(x) = \frac{1}{bh}\sum_{m=1}^{N} c_m \left[p(x+mh-0.5h) - p(x-mh+0.5h)\right], \tag{23b}$$

then

$$q(x-h) + aq(x) + q(x+h) = r(x). \tag{24}$$

$(2N)$ points are involved in the $(2N+2)$th-order implicit FD. For the known sequence $(p_{0.5}, p_{1.5}, \ldots, p_{M+0.5})$, which has $M+1$ points, the method of calculating its derivatives $(q_0, q_1, \ldots, q_{M+1})$ is introduced next. $q_N, q_{N+1}, \ldots, q_{M-N+1}$ are computed by the centred FD formulas,

$$q_{j-1} + a_N q_j + q_{j+1} = r_j, \ (j = N, N+2, \ldots, M-N+1), \tag{25}$$

where

$$q_j = q(jh), \tag{26a}$$

$$a_N = \frac{1}{b_N} - 2 \tag{26b}$$

and

$$r_j = \frac{\sum_{m=1}^{N} c_{N,m}(p_{j+m-0.5} - p_{j-m+0.5})}{b_N h}. \tag{26c}$$

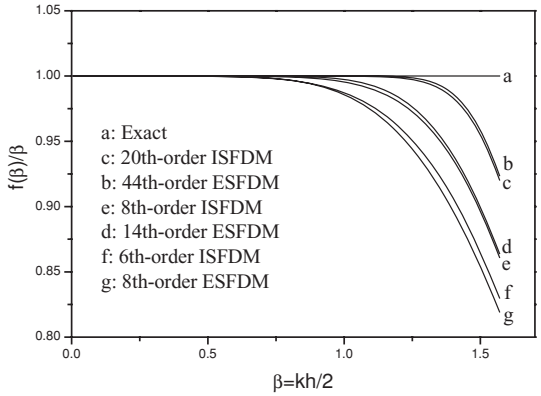

(a) Implicit 6th, 8th, 20th and explicit 8th, 14th, 44th -orders

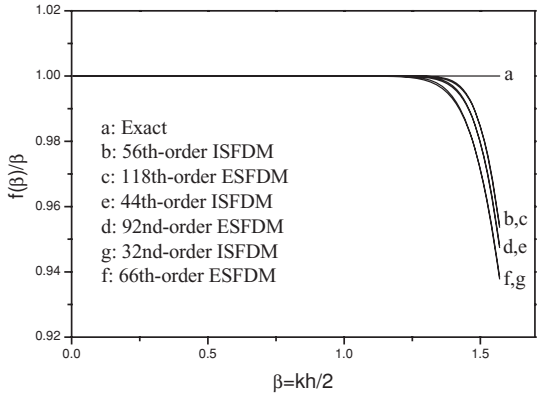

(b) Implicit 32nd, 44th, 56th and explicit 66th, 92nd, 118th -orders

Figure 3. Plot of $f_{\mathrm{ESFDM}}(\beta)/\beta$ and $f_{\mathrm{ISFDM}}(\beta)/\beta$ with the same accuracy. (a) Implicit 6th, 8th and 20th and explicit 8th, 14th and 44th orders. (b) Implicit 32nd, 44th and 56th and explicit 66th, 92nd and 118th orders.

If we assume that the known sequence ($p_{0.5}$, $p_{1.5}, \ldots, p_{M+0.5}$) is periodic, $q_0, q_1, \ldots, q_{N-1}, q_{M-N+2}, q_{M-N+3}, \ldots, q_{M+1}$ can also be calculated by centred FD formulas similar to eq. (25). Thus, tridiagonal equations can be formed from eq. (25) to determine the derivatives. For a non-periodic sequence, $q_0, q_1, \ldots, q_{N-1}, q_{M-N+2}, q_{M-N+3}, \ldots, q_{M+1}$ may be calculated by non-centred FD formulas to reach $(2N + 2)$th-order accuracy. However, the stability of non-centred FD is less than that of a centred FD scheme for a sequence with higher wavenumbers. Therefore, we adopt the centred FD formulas to calculate $q_1, q_2, \ldots, q_{N-1}$ and $q_M, q_{M-1}, \ldots, q_{M-N+2}$ using $4, 6, \ldots, (2N)$th-order accuracies, respectively, that is

$$q_{j-1} + a_j q_j + q_{j+1} = r_j, \ (j = 1, 2, \ldots, N-1) \tag{27a}$$

and

$$q_{j-1} + a_{M+1-j} q_j + q_{j+1} = r_j, \ (j = M-N+2, M-N+3, \ldots, M), \tag{27b}$$

where

$$a_j = \frac{1}{b_j} - 2, (j = 1, 2, \ldots, N-1) \tag{28a}$$

$$r_j = \frac{\sum_{m=1}^{j} c_{j,m}(p_{j+m-0.5} - p_{j-m+0.5})}{b_j h}, \ (j = 1, 2, \ldots, N-1), \tag{28b}$$

$$r_j = \frac{\sum_{m=1}^{M+1-j} c_{M+1-j,m}(p_{j+m-0.5} - p_{j-m+0.5})}{b_{M+1-j} h}, \ (j = M-N+2, M-N+3, \ldots, M) \tag{28c}$$

and $c_{j,1}, c_{j,2}, \ldots, c_{j,j}$ and b_j are the FD coefficients of the $(2j + 2)$th-order implicit difference formula.

Let

$$d_{j,m} = \frac{c_{j,m}}{b_j h}, \tag{29}$$

then

$$r_j = \begin{cases} \sum_{m=1}^{j} d_{j,m}(p_{j+m-0.5} - p_{j-m+0.5}) & (j = 1, 2, \ldots, N-1) \\ \sum_{m=1}^{N} d_{N,m}(p_{j+m-0.5} - p_{j-m+0.5}) & (j = N, N+1, \ldots, M-N+1) \\ \sum_{m=1}^{M+1-j} d_{M+1-j,m}(p_{j+m-0.5} - p_{j-m+0.5}) & (j = M-N+2, M-N+3, \ldots, M) \end{cases}. \tag{30}$$

Under the assumption of linear variation for p_0 and p_{M+1}, two equations are added as follows:

$$a_0 q_0 + q_1 = r_0 \tag{31a}$$

and

$$q_M + a_0 q_{M+1} = r_{M+1}, \tag{31b}$$

where

$$a_0 = a_1 + 1, \tag{32a}$$

$$r_0 = d_{1,1}\,(p_{1.5} - p_{0.5}) \tag{32b}$$

and

$$r_{M+1} = d_{1,1}\,(p_{M+0.5} - p_{M-0.5})\,. \tag{32c}$$

Then, the following tridiagonal matrix equations are formed to calculate the derivatives

$$\begin{bmatrix} a_0 & 1 & & & & & & & & & & & \\ 1 & a_1 & 1 & & & & & & & & & & \\ & 1 & a_2 & 1 & & & & & & & & & \\ & & \vdots & \vdots & \vdots & & & & & & & & \\ & & & 1 & a_{N-1} & 1 & & & & & & & \\ & & & & 1 & a_N & 1 & & & & & & \\ & & & & & \vdots & \vdots & \vdots & & & & & \\ & & & & & & 1 & a_N & 1 & & & & \\ & & & & & & & 1 & a_{N-1} & 1 & & & \\ & & & & & & & & \vdots & \vdots & \vdots & & \\ & & & & & & & & & 1 & a_2 & 1 & \\ & & & & & & & & & & 1 & a_1 & 1 \\ & & & & & & & & & & & 1 & a_0 \end{bmatrix} \begin{bmatrix} q_0 \\ q_1 \\ q_2 \\ \vdots \\ q_{M-1} \\ q_M \\ q_{M+1} \end{bmatrix} = \begin{bmatrix} r_0 \\ r_1 \\ r_2 \\ \vdots \\ r_{M-1} \\ r_M \\ r_{M+1} \end{bmatrix}. \tag{33}$$

4.1 A strategy to reduce computation in solving tridiagonal matrix equations

Assuming that the length of the sequence is M, conventional arithmetic for solving tridiagonal matrix equations approximately needs $3M$ multiplications, $2M$ divisions and $3M$ subtractions for real number operations and the need to visit the arrays $13M$ times (William *et al.* 1992).

In the numerical modelling, calculating derivatives with the same implicit difference format will be performed many times. Therefore, the repeat calculation involved in solving tridiagonal matrix equations can be pre-computed to reduce the overall computation. The coefficient vectors involved in solving tridiagonal matrix equations are also constant and can be pre-computed. Therefore, only $2M$ multiplications and subtractions and $8M$ visiting arrays are needed to solve the tridiagonal matrix equations.

Table 4. Homogeneous elastic model and its modelling parameters.

Parameters	Values
Model size	1000 m × 1000 m
Model *P*-wave velocity	2000 m s^{-1}
Model *S*-wave velocity	1000 m s^{-1}
Model density	1000 kg^3 m^{-3}
Grid size	10 m × 10 m
Time step	1 ms
P-wave source function	$-4\pi^2 f_p^2 t e^{-2\pi^2 f_p^2 t^2}$, $f_p = 25$hz
Source location	In the middle of the model

5 EXAMPLES OF NUMERICAL MODELLING

ESFDM and ISFDM are used to perform numerical modelling of the following 2-D elastic wave equations:

$$\frac{\partial v_x}{\partial t} = \frac{1}{\rho}\left(\frac{\partial \tau_{xx}}{\partial x} + \frac{\partial \tau_{xz}}{\partial z}\right), \tag{34a}$$

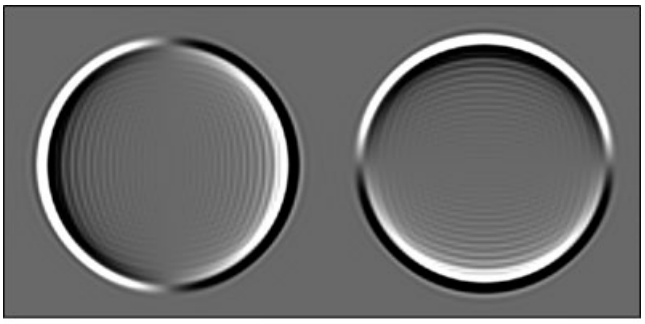

(a) 10th-order ESFDM

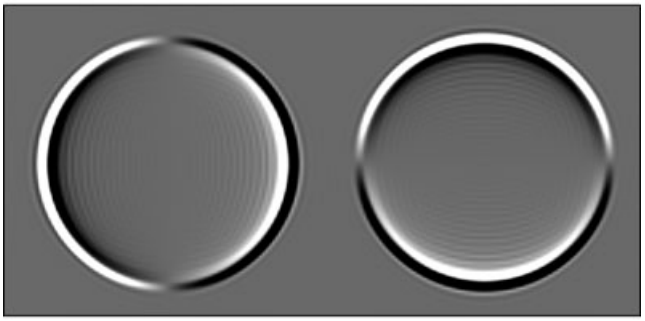

(b) 10th-order ISFDM

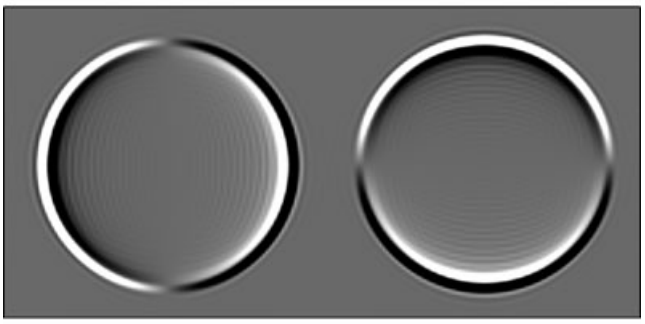

(c) 18th-order ESFDM

Figure 4. Snapshots of elastic wave equations numerical modelling, respectively, by ESFDM and ISFDM with different orders and pseudospectral method (left: x component; right: z component). (a) 10th-order ESFDM. (b) 10th-order ISFDM. (c) 18th-order ESFDM. (d) 18th-order ISFDM. (e) Pseudospectral method.

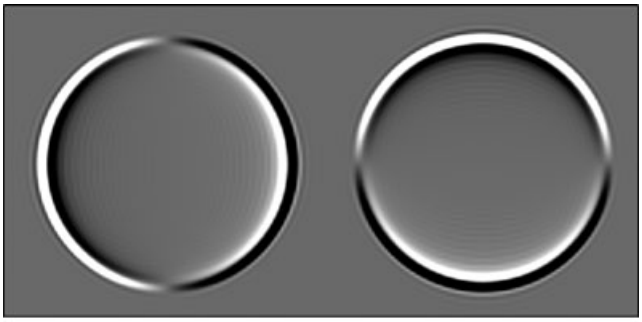

(d) 18th-order ISFDM

(e) Pseudospectral method

Figure 4. (*Continued.*)

$$\frac{\partial v_z}{\partial t} = \frac{1}{\rho}\left(\frac{\partial \tau_{xz}}{\partial x} + \frac{\partial \tau_{zz}}{\partial z}\right), \tag{34b}$$

$$\frac{\partial \tau_{xx}}{\partial t} = (\lambda + 2u)\frac{\partial v_x}{\partial x} + \lambda\frac{\partial v_z}{\partial z}, \tag{34c}$$

$$\frac{\partial \tau_{zz}}{\partial t} = \lambda\frac{\partial v_x}{\partial x} + (\lambda + 2u)\frac{\partial v_z}{\partial z} \tag{34d}$$

and

$$\frac{\partial \tau_{zx}}{\partial t} = \mu\left(\frac{\partial v_z}{\partial x} + \frac{\partial v_x}{\partial z}\right). \tag{34e}$$

In these equations, (v_x, v_z) is the velocity vector, $(\tau_{xx}, \tau_{zz}, \tau_{xz})$ is a vector containing three components of stress, $\lambda(x, z)$ and $\mu(x, z)$ are the Lame coefficients and $\rho(x, z)$ is the density. We perform ESFDM and ISFDM on the classic staggered grids (Virieux 1986). In the modelling, the first-order space derivatives are calculated by ESFDM and ISFDM, respectively, and the time derivatives by explicit 2nd-order FD.

5.1 Numerical modelling of a homogeneous model

Numerical modelling is performed based on the model and computation parameters shown in Table 4. Snapshots at 200 ms, respectively, by ISFDM and ESFDM with different orders and PSM are shown in Fig. 4. The figure demonstrates that the accuracy of FD modelling increases with the increase of order and the precision of the 10th-order ISFDM is greater than that of a 10th-order ESFDM and is nearly identical

Table 5. Average CPU time per time step of numerical simulating by ESFDM and ISFDM for a homogeneous elastic model with different size.

Model size	Average CPU time of 10th-order ESFDM (ms/time step)	Average CPU time of 18th-order ESFDM (ms/time step)	Average CPU time of 10th-order ISFDM (ms/time step)
1000 m × 1000 m	8.8	10.8	7.6
2000 m × 2000 m	66.2	99.6	79.6
3000 m × 3000 m	184.4	321.8	254.2

Modelling parameters are listed in Table 4; maximum time is 500 ms.

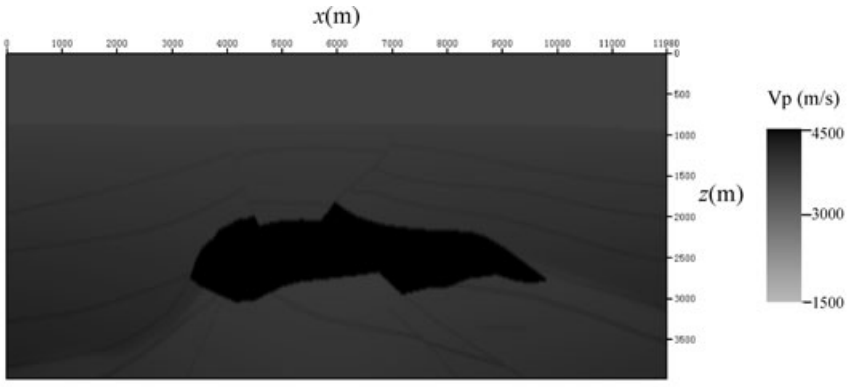

(a) SEG/EAGE salt model (S-wave velocity and density, having the similar characteristics to P-wave velocity, are not shown)

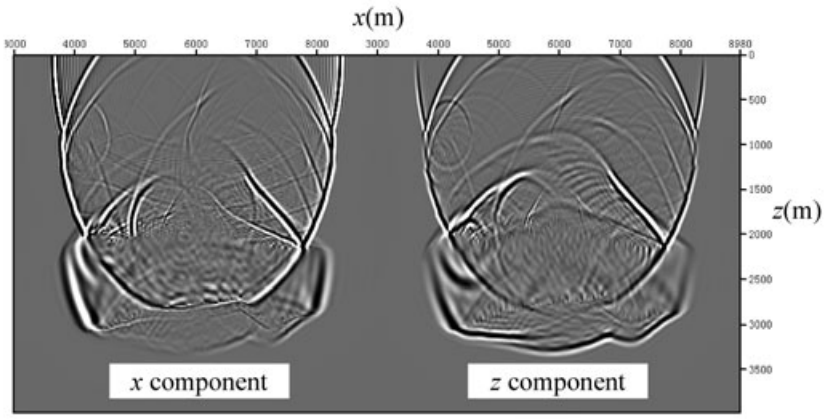

(b) Snapshots of *x* (left) and *z* (right) components at t=1600ms by 20th-order ESFDM

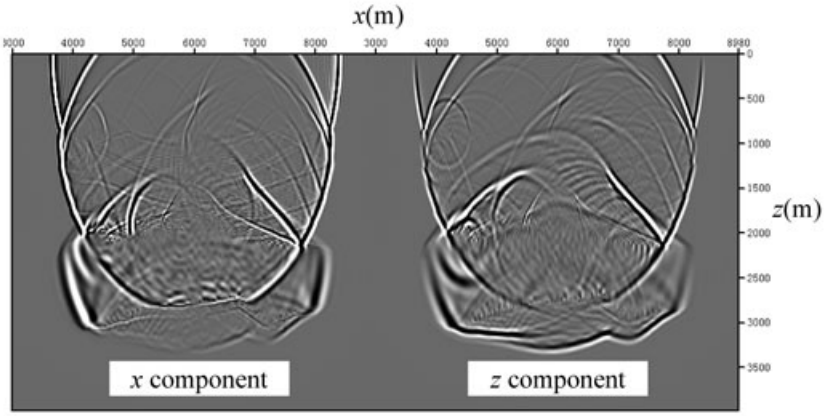

(c) Snapshots of *x* (left) and *z* (right) components at t=1600ms by 20th-order ISFDM

Figure 5. Numerical modelling results of SEG/EAGE salt model, respectively, by 20th-order ESFDM, 20th-order ISFDM and pseudospectral method. (a) SEG/EAGE salt model (*S*-wave velocity and density, having the similar characteristics to *P*-wave velocity, are not shown). (b) Snapshots of *x* (left) and *z* (right) components at $t = 1600$ ms by 20th-order ESFDM. (c) Snapshots of *x* (left) and *z* (right) components at $t = 1600$ ms by 20th-order ISFDM. (d) Snapshots of *x* (left) and *z* (right) components at $t = 1600$ ms by pseudospectral method. (e) OBC gather of *x* (left) and *z* (right) components by 20th-order ESFDM. (f) OBC gather of *x* (left) and *z* (right) components by 20th-order ISFDM. (g) OBC gather of *x* (left) and *z* (right) components by pseudospectral method.

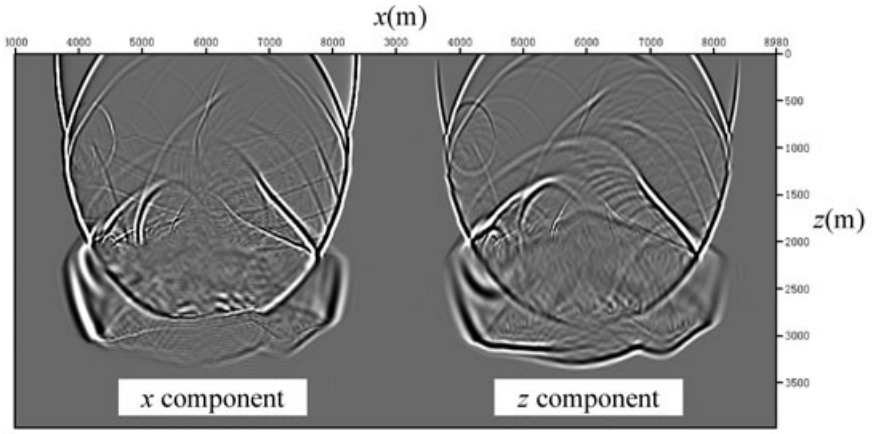

(d) Snapshots of x (left) and z (right) components at t=1600ms by pseudo-spectral method

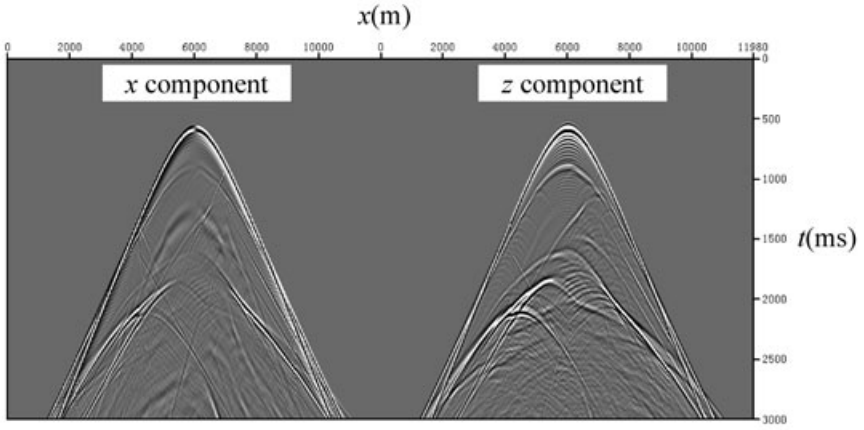

(e) OBC gather of x (left) and z (right) components by 20th-order ESFDM

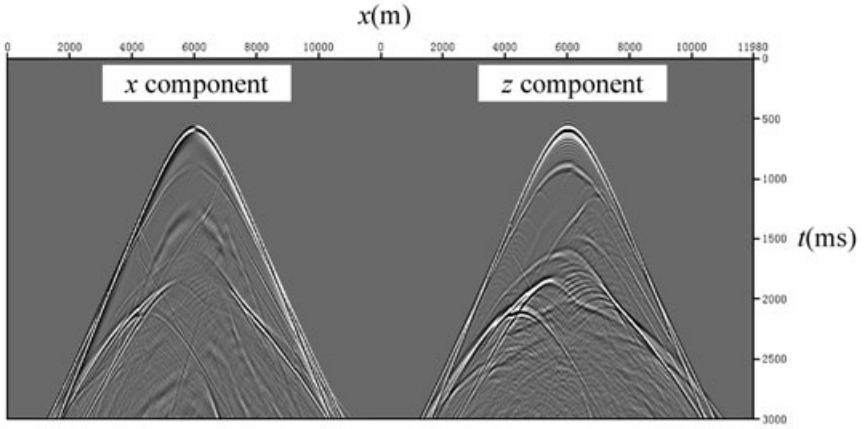

(f) OBC gather of x (left) and z (right) components by 20th-order ISFDM

Figure 5. (*Continued.*)

to that of an 18th-order ESFDM. In addition, we record CPU time of numerical simulating by the 10th-order ESFDM, 18th-order ESFDM and 10th-order ISFDM for a homogeneous elastic model with different sizes for 500 time steps. The results for average CPU time per time step are shown in Table 5, which demonstrates that a 10th-order ISFDM costs less CPU time than an 18th-order ESFDM and thus is more efficient.

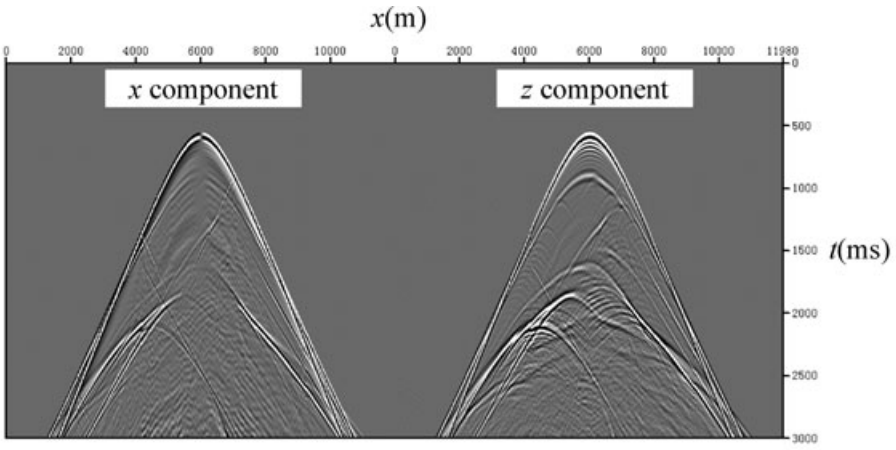

(g) OBC gather of x (left) and z (right) components by pseudo-spectral method

Figure 5. (*Continued.*)

Table 6. SEG/EAGE salt model and its simulating parameters.

Parameters	Values
Model size	12 000 m × 4000 m
Model first layer	Ocean water
Grid size	20 m × 20 m
Time step	1 ms
P-wave source function	Sine signal of 20 Hz with one-period length
Source location	$x_0 = 6000$, $z_0 = 20$
Receiver location	Ocean bottom

5.2 Numerical modelling of the SEG/EAGE salt model

Finally, numerical modelling of the elastic wave equations, respectively, by the 20th-order ESFDM, 20th-order ISFDM and PSM, is utilized to simulate wave propagation in the Society of Exploration Geophysicists/European Association of Geoscientists and Engineers (SEG/EAGE) salt model. Here, we simply extend the model spatially to avoid reflections from the top and other edges of the model. Fig. 5(a) shows the model, and Table 6 lists the model and its simulation parameters. Snapshots and shot gathers are illustrated in Figs 5(b)–(g). The results demonstrate that the accuracy of our ISFDM is greater than that of ESFDM for the same order. For simulation of 3000 time steps for a model comprising 600 × 200 grids, the CPU time of modelling by the 20th-order ESFDM, 40th-order ESFDM and 20th-order ISFDM is about 492 s, 784 s and 598 s, respectively. Therefore, a 20th-order ISFDM, which has almost the same accuracy as that of a 40th-order ESFDM, costs less computation time and is therefore clearly more efficient.

6 DISCUSSION

First, we compare the computations required by ESFDM and ISFDM. Since the derivative calculation is performed many times in a numerical modelling, the computation time for difference coefficients can be ignored in the following analysis. Assuming that the length of the sequence is M, the derivatives of the sequence are calculated K times and the $(2N)$th-order ESFDM and $(2N + 2)$th-order ISFDM are adopted, then ESFDM costs nearly $N \times M \times K$ multiplications, $2N \times M \times K$ additions and $4N \times M \times K$ visiting arrays and ISFDM costs nearly $(N +$

Table 7. Computation amount comparison of $(2N)$th-order ESFDM and $(2N + 2)$th-order ISFDM.

Operation	Operation times of $(2N)$th-order ESFDM $(M \times K)$	Operation times of $(2N + 2)$th-order ISFDM $(M \times K)$
×	N	$N + 2$
+ or −	$2N$	$2N + 2$
Visiting array elements	$4N$	$4N + 8$

The length of the sequence is M; the derivatives of the sequence are calculated K times.

Table 8. Accuracy relationship between ESFDM and ISFDM under the condition of the same computation amount.

N	$(2N+4)$th-order ESFDM	$(2N+2)$th-order ISFDM (Costing the same computation amount as $(2N+4)$th-order ESFDM)	$(4N)$th-order ESFDM (Reaching nearly the same accuracy as $(2N+2)$th-order ISFDM)
2	8	6	8 (8)
3	10	8	12 (14)
5	15	12	20 (22)
10	24	22	40 (44)
20	44	42	80 (86)
30	64	62	120 (130)

The numbers shown in the parentheses of the last column are the ESFDM orders that $(2N+2)$th-order ISFDM can really reach. Additional cost of visiting arrays, which may be dependent on computer configuration and programming language, is not considered here.

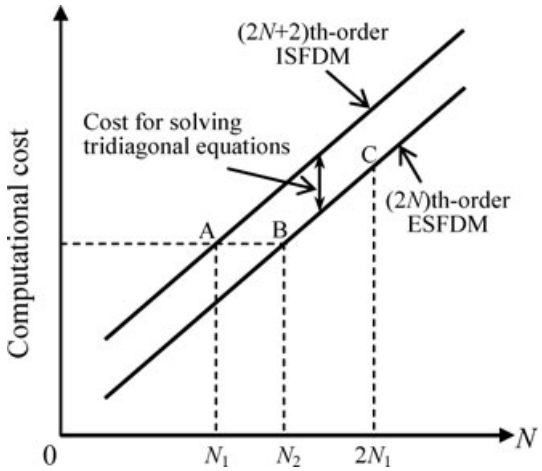

Figure 6. Relationship between ISFDM and ESFDM for the accuracy and the computational cost. The computational cost of the $(2N+2)$th-order ISFDM is equal to that of the $(2N)$th-order ESFDM plus that of solving tridiagonal equations (constant for the fixed sequence length). The $(2N_1+2)$th-order ISFDM (point A), having the same computational cost as the $(2N_2)$th-order ESFDM (point B), reaches the accuracy of the $(4N_1)$th-order ESFDM (point C). The $(2N_2)$th-order ESFDM may be replaced by the $(2N_1+2)$th-order ISFDM.

$2) \times M \times K$ multiplications, $(2N+2) \times M \times K$ additions or subtractions and $(4N+8) \times M \times K$ visiting arrays, as shown in Table 7. For ISFDM, only additional memory of $2M$ real numbers is needed for saving the coefficient vectors involved in solving tridiagonal equations; this can be ignored. Since additional cost of visiting arrays may be dependent on computer configuration and programming language, it is not considered here and thus a $(2N+2)$th-order ISFDM requires nearly the same amount of computation as a $(2N+4)$th-order ESFDM. Therefore, under the condition of the same amount of calculation, a $(2N+4)$th-order ESFDM may be replaced by a $(2N+2)$th-order ISFDM, which attains the accuracy of a $(4N)$th-order ESFDM. This relationship is also shown in Table 8.

In our numerical modelling example, we find that a $(2N+2)$th-order ISFDM requires more CPU time than a $(2N)$th-order ESFDM. The reason is that this ISFDM visits more arrays than this ESFDM and visiting array element requires more time than visiting a variable in the running of a computer program. Table 7 shows that the computation cost of the $(2N+2)$th-order ISFDM is equal to that of the $(2N)$th-order ESFDM plus that of solving tridiagonal equations. For the fixed sequence length in the wave equation modelling, solving tridiagonal equations requires nearly the same time; therefore, the difference between the computational cost of the $(2N+2)$th-order ISFDM and that of the $(2N)$th-order ESFDM will be approximately a constant. Indicated by eq. (1) and Table 7, the computational cost of the $(2N)$th-order ESFDM linearly varies with N and so does the ISFDM. Fig. 6 shows the relationship between ISFDM and ESFDM for the accuracy and the computation cost. From this figure, we clearly note that some-order ISFDM may be found and used to replace the given-order ESFDM. For example, for the ESFDM of a given $(2N_2)$th order (point B), the $(2N_1+2)$th order ISFDM with the same computational cost may be found in point A. This ISFDM will attain the accuracy of the $(4N_1)$th-order ESFDM (point C). If $4N_1$ is greater than $2N_2$, this ESFDM can be replaced by this ISFDM. However, it is difficult to give generally specific relationships between N_1 and N_2 because the CPU time is determined by the speed of arithmetic operations, visiting arrays, etc., which depend on computer configuration and programming language.

7 CONCLUSIONS

The explicit FD technique is commonly used in seismic modelling because of its relatively small computation time requirement. Implicit FDs are usually considered expensive due to the requirement of solving more equations and thus are not generally popular. In this paper, we have developed implicit staggered-grid FD formulas with any order of accuracy for first-order derivatives. This method involves solving tridiagonal matrix equations. For calculating derivatives with the same FD format many times, the $(2N + 2)$th-order implicit staggered-grid method requires nearly the same amount of computation and occupies nearly the same amount of memory as those of a $(2N + 4)$th-order explicit staggered-grid method but attains the accuracy of a $(4N)$th-order explicit staggered-grid method when additional cost of visiting arrays is not considered. We conclude that a high-order explicit staggered-grid method may be replaced by implicit staggered-grid method of some order, which will increase the accuracy but not the cost of computation. Thus, this implicit method can be used to simulate 1-D, 2-D and 3-D acoustic and elastic wave propagation. It can also be extended to the rotated staggered-grid modelling.

ACKNOWLEDGEMENTS

We thank the editor Dr. Johan Robertsson and two anonymous reviewers for constructive criticism of our paper. YL would like to thank China Scholarship Council for their financial support for this research and University of Texas at Austin, Institute of Geophysics for providing with the facilities. This research is also partially supported by the National '863' Program of China under contract no. 2007AA06Z218.

REFERENCES

Abokhodair, A.A., 2009. Complex differentiation tools for geophysical inversion, *Geophysics,* **74**, H1–H11.

Aoi, S. & Fujiwara, H., 1999. 3-D finite-difference method using discontinuous grids, *Bull. Seism. Soc. Am.,* **89**, 918–930.

Bansal, R. & Sen, M.K., 2008. Finite-difference modelling of S-wave splitting in anisotropic media, *Geophys. Prospect.,* **56**, 293–312.

Bohlen, T., 2002. Parallel 3-D viscoelastic finite-difference seismic modeling, *Comput. Geosci.,* **28**, 887–899.

Bohlen, T. & Saenger, E.H., 2006. Accuracy of heterogeneous staggered-grid finite-difference modeling of Rayleigh waves, *Geophysics,* **71**, T109–T115.

Boersma, B.J., 2005. A staggered compact finite difference formulation for the compressible Navier–Stokes equations, *J. Comput. Phys.,* **208**, 675–690.

Claerbout, J.F., 1985. The craft of wavefield extrapolation, in *Imaging the Earth's Interior*, pp. 260–265, Blackwell Scientific Publications, Oxford.

Crase, E., 1990. High-order (space and time) finite-difference modeling of the elastic wave equation, *SEG Expanded Abstracts,* **9,** 987–991.

Dablain, M.A., 1986. The application of high-order differencing to the scalar wave equation, *Geophysics,* **51**, 54–66.

De Basabe, J.D. & Sen, M.K., 2007. Grid dispersion and stability criteria of some common finite-element methods for acoustic and elastic wave equations, *Geophysics,* **72**(6), T81–T95.

De Basabe, J.D. & Sen, M.K., 2009. New developments in finite element methods of seismic modeling, *The Leading Edge,* **28**, 562–567.

De Basabe, J.D., Sen, M.K. & Wheeler, M.F., 2008. The interior penalty discontinuous Galerkin method for elastic wave propagation: grid dispersion, *Geophys. J. Int.,* **175**, 83–93.

Ekaterinaris, J.A., 1999. Implicit, high-resolution compact schemes for gas dynamics and aeroacoustics, *J. Comput. Phys.,* **156**, 272–299.

Emerman, S., Schmidt, W. & Stephen, R., 1982. An implicit finite-difference formulation of the elastic wave equation, *Geophysics,* **47**, 1521–1526.

Etgen, J.T. & O'Brien, M.J., 2007. Computational methods for large-scale 3D acoustic finite-difference modeling: a tutorial, *Geophysics,* **72**, SM223–SM230.

Fei, T. & Liner, C.L., 2008. Hybrid Fourier finite difference 3D depth migration for anisotropic media, *Geophysics,* **73**, S27–S34.

Fornberg, B., 1987. The pseudospectral method comparisons with finite differences for the elastic wave equation, *Geophysics,* **52**, 483–501.

Gottschämer, E. & Olsen, K., 2001. Accuracy of the explicit planar free surface boundary condition implemented in a fourth-order staggered-grid velocity-stress finite-difference scheme, *Bull. Seism. Soc. Am.,* **91**, 617–623.

Graves, R.W., 1996. Simulating seismic wave propagation in 3D elastic media using staggered-grid finite differences, *Bull. Seism. Soc. Am.,* **86**, 1091–1106.

Hayashi, K. & Burns, D.R., 1999. Variable grid finite-difference modeling including surface topography, *SEG Expanded Abstracts,* **18,** 523–527.

Hayashi, K., Burns, D.R. & Toksöz, M.N., 2001. Discontinuous-grid finite-difference seismic modeling including surface topography, *Bull. Seism. Soc. Am.,* **91**, 1750–1764.

Hestholm, S., 2003. Elastic wave modeling with free surfaces: stability of long simulations, *Geophysics,* **68**, 314–321.

Hestholm, S., 2007. Acoustic VTI modeling using high-order finite-differences, *SEG Expanded Abstracts,* **26,** 139–142.

Hestholm, S. & Ruud, B., 1998. 3-D finite-difference elastic wave modeling including surface topography, *Geophysics,* **63**, 613–622.

Igel, H., Mora, P. & Riollet, B., 1995. Anistotropic wave propagation through finite-difference grids, *Geophysics,* **60**, 1203–1216.

Käser, M. & Dumbser, M., 2006. An arbitrary high-order discontinuous Galerkin method for elastic waves on unstructured meshes—I. The two-dimensional isotropic case with external source terms, *Geophys. J. Int.,* **166**, 855–877.

Kelly, K.R., Ward, R., Treitel, W.S. & Alford, R.M., 1976. Synthetic seismograms: a finite-difference approach, *Geophysics,* **41**, 2–27.

Kindelan, M., Kamel, A. & Sguazzero, P., 1990. On the construction and efficiency of staggered numerical differentiators for the wave equation, *Geophysics,* **55**, 107–110.

Komatitsch, D. & Vilotte, J., 1998. The spectral element method: an efficient tool to simulate the seismic response of 2D and 3D geological structures, *Bull. Seism. Soc. Am.,* **88**, 368–392.

Kosloff, D., Pestana, R. & Tal-Ezer, H., 2008. Numerical solution of the constant density acoustic wave equation by implicit spatial derivative operators, *SEG Expanded Abstracts,* **27,** 2057–2061.

Krüger, O.S., Saenger, E.H. & Shapiro, S., 2005. Scattering and diffraction by a single crack: an accuracy analysis of the rotated staggered grid, *Geophys. J. Int.,* **162**, 25–31.

Larner, K. & Beasley, C., 1987. Cascaded migrations-improving the accuracy of finite-difference migration, *Geophysics,* **52**, 618–643.

Lee, C. & Seo, Y., 2002. A new compact spectral scheme for turbulence simulations, *J. Comput. Phys.,* **183**, 438–469.

Lele, S.K., 1992. Compact finite difference schemes with spectral-like resolution, *J. Comput. Phys.,* **103**, 16–42.

Levander, A., 1988. Fourth-order finite-difference P-SV seismograms, *Geophysics,* **53**, 1425–1436.

Li, Z., 1991. Compensating finite-difference errors in 3-D migration and modeling, *Geophysics,* **56**, 1650–1660.

Liu, Y. & Wei, X.C., 2008. Finite-difference numerical modeling with even-order accuracy in two-phase anisotropic media, *App. Geophys.,* **5**, 107–114.

Lombard, B., Piraux, J., Gélis, C. & Virieux, J., 2008. Free and smooth boundaries in 2D FD schemes transient elastic waves, *Geophys. J. Int.,* **172**, 252–261.

Madariaga, R., 1976. Dynamics of an expanding circular fault, *Bull. Seism. Soc. Am.,* **66**, 639–666.

Meitz, H.L. & Fasel, H.F., 2000. A compact-difference scheme for the Navier–Stokes equations in vorticity-velocity formulation, *J. Comput. Phys.,* **157**, 371–403.

Meyer, C.D., 2000. Determinants, in *Matrix Analysis and Applied Linear Algebra*, p. 486, SIAM Press, Philadelphia, PA.

Mittet, R., 2002. Free-surface boundary conditions for elastic staggered-grid modeling schemes, *Geophysics,* **67**, 1616–1623.

Moczo, P., Kristek, J. & Halada, L., 2000. 3D fourth-order staggered-grid finite-difference schemes: stability and grid dispersion, *Bull. Seism. Soc. Am.,* **90**, 587–603.

Moczo, P., Kristek, J., Vavrycuk, V., Archuleta, R. & Halada, L., 2002. Heterogeneous staggered-grid finite-difference modeling of seismic motion with volume harmonic and arithmetic averaging of elastic moduli and densities, *Bull. Seism. Soc. Am.,* **92**, 3042–3066.

Nihei, T. & Ishii, K., 2003. A fast solver of the shallow water equations on a sphere using a combined compact difference scheme, *J. Comput. Phys.,* **187**, 639–659.

Ohminato, T. & Chouet, B.A., 1997. A free-surface boundary condition for including 3D topography in the finite-difference method, *Bull. Seism. Soc. Am.,* **87**, 494–515.

Operto, S., Virieux, J., Amestoy, P., L'Excellent, J.Y., Giraud, L. & Ali, H.B.H., 2007. 3D finite-difference frequency-domain modeling of visco-acoustic wave propagation using a massively parallel direct solver: A feasibility study, *Geophysics,* **72**, SM195–SM211.

Opršal, I. & Zahradník, J., 1999. Elastic finite-difference method for irregular grids, *Geophysics,* **64**, 240–250.

Pei, Z., 2004. Numerical modeling using staggered-grid high order finite-difference of elastic wave equation on arbitrary relief surface, *Oil Geophys. Prosp.* (abstract in English), **39**, 629–634.

Pitarka, A., 1999. 3D elastic finite-difference modeling of seismic motion using staggered grids with nonuniform spacing, *Bull. Seism. Soc. Am.,* **89**, 54–68.

Pratt, R.G., Shin, C. & Hicks, G.J., 1998. Gauss-Newton and full Newton methods in frequency-space seismic waveform inversion, *Geophys. J. Int.,* **133**, 341–362.

Ravaut, C., Operto, S., Improta, L., Virieux, J., Herrero, A. & Dell'Aversana, P., 2004. Multiscale imaging of complex structures from multifold wide-aperture seismic data by frequency-domain full-waveform tomography: application to a thrust belt, *Geophys. J. Int.,* **159**, 1032–1056.

Rivière, B. & Wheeler, M., 2003. Discontinuous finite element methods for acoustic and elastic wave problems, *Contemp. Math.,* **329**, 271–282.

Ristow, D. & Ruhl, T., 1994. Fourier finite-difference migration, *Geophysics,* **59**, 1882–1893.

Ristow, D. & Ruhl, T., 1997. 3-D implicit finite-difference migration by multiway splitting, *Geophysics,* **62**, 554–567.

Robertsson, J.O.A., Blanch, J. & Symes, W., 1994. Viscoelastic finite-difference modeling, *Geophysics,* **59**, 1444–1456.

Robertsson, J.O.A., 1996. A numerical free-surface condition for elastic/viscoelastic finite-difference modeling in the presence of topography, *Geophysics,* **61**, 1921–1934.

Rojas, O., Day, S., Castillo, J. & Dalguer, L.A., 2008. Modelling of rupture propagation using high-order mimetic finite differences, *Geophys. J. Int.,* **172**, 631–650.

Saenger, E.H. & Bohlen, T., 2004. Finite-difference modeling of viscoelastic and anisotropic wave propagation using the rotated staggered grid, *Geophysics,* **69**, 583–591.

Saenger, E.H. & Shapiro, S.A., 2002. Effective velocities in fractured media: a numerical study using the rotated staggered finite difference grid, *Geophys. Prospect.,* **50**, 183–194.

Saenger, E.H., Gold, N. & Shapiro, S.A., 2000. Modeling the propagation of elastic waves using a modified finite-difference grid, *Wave Motion,* **31**, 77–92.

Saenger, E.H., Ciz, R., Krüger, O.S., Schmalholz, S.M., Gurevich, B. & Shapiro, S.A., 2007. Finite-difference modeling of wave propagation on microscale: a snapshot of the work in progress, *Geophysics,* **72**, SM293–SM300.

Shan, G., 2007. Optimized implicit finite-difference migration for TTI media, *SEG Expanded Abstracts,* **26,** 2290–2293.

Tessmer, E., 2000. Seismic finite-difference modeling with spatially varying time steps, *Geophysics,* **65**, 1290–1293.

Virieux, J., 1984. SH-wave propagation in heterogeneous media: velocity-stress finite-difference method, *Geophysics,* **49**, 1933–1957.

Virieux, J., 1986. P-SV wave propagation in heterogeneous media: velocity stress finite difference method, *Geophysics,* **51**, 889–901.

Vossen, V.R., Robertsson, J.O.A. & Chapman, C., 2002. Finite-difference modeling of wave propagation in a fluid-solid configuration, *Geophysics,* **67**, 618–624.

Wang, Y. & Schuster, G.T., 1996. Finite-difference variable grid scheme for acoustic and elastic wave equation modeling, *SEG Expanded Abstracts,* **15,** 674–677.

William, H.P., Brian, P.F., Saul, A.T. & William, T.V., 1992. *Numerical Recipes in FORTRAN*, 2nd edn, Cambridge University Press, Cambridge, England.

Zhang, H. & Zhang, Y., 2007. Implicit splitting finite difference scheme for multi-dimensional wave simulation, *SEG Expanded Abstracts,* **26,** 2011–2014.

Zhang, G., Zhang, Y. & Zhou, H., 2000. Helical finite-difference schemes for 3-D depth migration, *SEG Expanded Abstracts,* **19,** 862–865.